Switchable ionic conductivity and viscoelasticity of ionogels containing photo- and thermo-responsive organometallic ionic liquids

Sumitani, Ryo

Mochida, Tomoyuki

(Citation)
Journal of Molecular Liquids,342:117510

(Issue Date)
2021-11-15

(Resource Type)
journal article

(Version)
Accepted Manuscript

(URL)
https://hdl.handle.net/20.500.14094/90008685

Switchable Ionic Conductivity and Viscoelasticity of Ionogels Containing Photo- and Thermo-Responsive Organometallic Ionic Liquids

Ryo Sumitani,[a] Tomoyuki Mochida*[a,b]

[a]*Department of Chemistry, Graduate School of Science, Kobe University, 1-1 Rokkodai, Nada, Kobe, Hyogo 657-8501, Japan*

[b]*Research Center for Membrane and Film Technology, Kobe University, 1-1 Rokkodai, Nada, Kobe, Hyogo 657-8501, Japan*

**Corresponding author. E-mail address: tmochida@platinum.kobe-u.ac.jp*

ORCID-ID: 0000-0002-6617-2994 (Sumitani), 0000-0002-3446-2145 (Mochida)

Abstract

Ionic liquid gels (ionogels) are useful as flexible solid electrolytes owing to their high ionic conductivity and non-volatility. Ionogels possessing photoswitchable ionic conductivity have versatile electronic applications, although the fabrication of such materials remains a challenge. Herein, we synthesized photoresponsive ionogels by adding a low-molecular-weight gelator, 12-hydroxystearic acid, to photoreactive organometallic ionic liquids. UV photoirradiation of an ionogel containing an ionic liquid $[Ru(C_5H_5)(C_6H_5OC_3H_6CN)][N(SO_2F)_2]$ (**Gel-1**) decreased its ionic conductivity while increasing its viscoelastic modulus. This is owing to the photochemical formation of coordination bonds between the ionic liquid cations in the gel. The reaction was reversed upon heating, hence the physical properties were reversibly controlled by the application of light and heat. An ionogel containing an ionic liquid $[Ru(C_5H_5)\{C_6H_3(OC_6H_{12}CN)_3\}][N(SO_2F)_2]$ with three substituents (**Gel-2**) was also prepared, which was transformed into a rubber-like solid having a coordination polymer structure upon photoirradiation. The photoproduct exhibited much lower ionic conductivity and higher viscoelastic modulus compared with the photoproduct of **Gel-1**.

Keywords: ionic liquid; ionogel; ruthenium complex; sandwich complex; ionic conductivity; viscoelasticity

1. Introduction

There have been extensive studies on their synthesis and application of ionic liquids (ILs) recently [1]. Owing to their characteristic properties, such as negligible vapor pressure, flame retardancy, and high ionic conductivity, ILs are promising for electrochemical applications, such as fuel cells [2,3], solar cells [4,5], batteries [6], and sensors [7]. Recently, a number of studies have been conducted on IL-based solid electrolytes, which are generally fabricated by gelation [8–11] or polymerization [12–15] of ILs. Ionic liquid gels (ionogels) have typically been prepared by incorporating low-molecular-weight gelators [16–21], silica nanoparticles [22,23], supermolecular polymers [24,25], or covalently bonded polymers [26,27] into ILs. Furthermore, stimuli-responsive ionogels have been designed to respond to temperature changes [28–32], pH changes [33,34], ionic species [35], light [36–45], electric fields [46], and magnetic fields [47]. They exhibit interesting switching phenomena, such as ionic conductivity alteration, structural transformation, gel–sol transition, and volume phase transition in response to external stimuli.

Controlling the electronic properties of ionogels via external stimuli, particularly via photoirradiation, is useful for novel switchable electronic devices. However, there are very few examples of ionogels that exhibit photocontrollable conductivity. The ionic conductivity of photoisomerizable ionogels varies upon photoirradiation [41], although the variation is small. A photo-triggered gel–sol transition accompanies a larger variation [42], although the sol state is less favorable for electronic devices. Most of the photoresponsive ionogels reported so far contain photochromic molecules such as azobenzene in the gelator or polymer framework, which facilitate the viscoelastic changes or gel–sol transitions by photoisomerization [42–44].

Additionally, photoresponsive gels can be synthesized from ILs containing photoresponsive moieties, although very few examples are available because of their high melting points [45].

This study aims to develop ionogels whose ionic conductivity and viscoelasticity can be reversibly controlled by the application of light and heat. We previously reported the synthesis and properties of photoreactive ILs containing cationic sandwich-type ruthenium complexes, which undergo coordination transformation in response to external stimuli [48–52]. The ILs shown in Fig. 1, $[Ru(C_5H_5)(C_6H_5OC_3H_6CN)]FSA$ (**IL-1**) and $[Ru(C_5H_5)\{C_6H_3(OC_6H_{12}CN)_3\}]FSA$ (**IL-2**) (where FSA = $N(SO_2F)_2$), transformed into a highly viscous oligomer-containing liquid and an amorphous solid coordination polymer, respectively, upon UV photoirradiation [48,49]. In these reactions, the photodissociation of the arene ligand is followed by the coordination of three CN groups to each Ru ion to form intermolecular bonds between the cations. The reactions were reversed upon heating. These ILs are suitable for producing the desired ionogels because these reactions are accompanied by reversible changes in the ionic conductivity caused by the application of light and heat [48,49].

In this paper, we report the syntheses and properties of ionogels **Gel-1** and **Gel-2**, which are physical gels formed from **IL-1** and **IL-2**, respectively. 12-hydroxystearic acid (12-HSA, Fig. 2a), which is a typical low-molecular-weight gelator used for gelation of edible oils and ILs [53,54], was used as the gelator in this work. Upon UV photoirradiation, the viscoelasticity of **Gel-1** increased, whereas **Gel-2** turned into a rubber-like solid, and the ionic conductivities of the two gels were reversibly controllable by the application of light and heat (Fig. 2b). The changes in the physical properties associated with these reactions were evaluated by differential scanning calorimetry (DSC), dynamic rheology, and ionic conductivity measurements, and are described in the following sections.

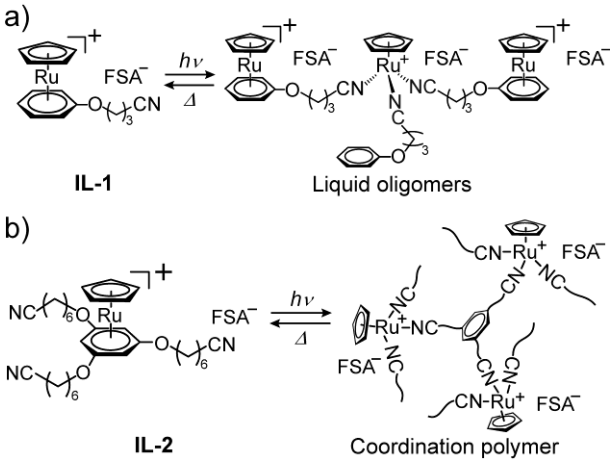

Fig. 1. Reversible formation of (a) liquid oligomers and (b) coordination polymer from ruthenium-containing ionic liquids **IL-1** [49] and **IL-2** [48]. FSA^- denotes the bis(fluorosulfonyl)amide anion. The product of the reaction in a) is a mixture of oligomers.

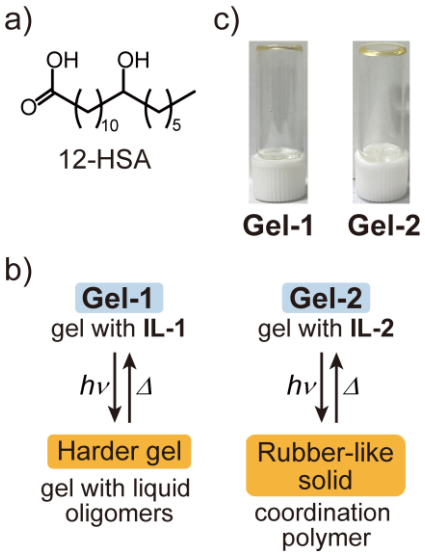

Fig. 2. (a) Structural formula of the gelator used in this study. (b) The reactivities of **Gel-1** and **Gel-2**. (c) Photographs of the ionogels.

2. Results and Discussion

2.1. Synthesis and Properties of the Ionogels

Gel-1 and **Gel-2** were formed by adding 12-HSA (5 wt%) to **IL-1** or **IL-2**, followed by heating to 120 °C and subsequent cooling to ambient temperature (Fig. 2c). They were pale yellow soft gels, exhibiting glass transitions at –60 and –54 °C, respectively, as revealed by

DSC (Fig. S1). These temperatures are identical to the glass transition temperatures of the constituent ILs [48,55]. In both cases, gel–sol transitions were observed in the DSC traces at 73 °C and 66 °C upon heating and cooling, respectively. The gel–sol transition behavior was similar to that exhibited by an organogel composed of 12-HSA (7 wt%) and dodecane upon heating at 70 °C [56].

Although pure liquid **IL-1** does not crystallize [55], the IL in **Gel-1** underwent cold crystallization at approximately –10 °C (Fig. S1a). This feature did not influence the characterization of the materials described below, which were conducted at ambient temperature or higher. The crystallized IL in **Gel-1** melted at 26 °C, which is consistent with its glass transition temperature (–60 °C) in terms of the empirical relationship for molecular liquids ($T_g/T_m = 2/3$) [57]. **Gel-2** exhibited no crystallization.

*2.2. Reactivities of **Gel-1***

Upon UV photoirradiation, pale yellow **Gel-1** changed to a yellow gel having a higher viscoelasticity in a few minutes. Heating the photoproduct at 120 °C for 1 min yielded the original gel. This reaction cycle was repeatable.

Upon UV photoirradiation (365 nm, LED), **Gel-1** changed to a yellow gel within a few minutes, owing to the photochemical formation of oligomer cations, as shown in Fig. 1a. The temporal evolution of the reaction determined from the UV-Vis and ^{1}H NMR spectra is shown in Fig. 3a. The reaction was 70% complete at 3 min and 90% complete at 10 min, following which it became constant. The spectral changes upon photoirradiation were identical to those observed for **IL-1** [49]. The reaction undergone by **IL-1** under identical conditions is shown in the figure as well. The reaction of **Gel-1** was slightly faster than that of **IL-1**, which is probably attributable to the effect of efficient light scattering inside the gel. The photoproduct returned

to its original gel state following heating at 120 °C for 1 min and subsequently cooling to ambient temperature (Fig. S2a). The photochemical and thermal reaction cycles were repeatable.

The viscoelastic changes upon photoirradiation were evaluated using dynamic rheological measurements (Fig. 4a). In the measured angular frequency range, the storage modulus (G') exceeded the loss modulus (G'') before and after photoirradiation (strain 0.1%). Both G' and G'' were nearly independent of the angular frequency, indicating a viscoelastic solid-like behavior. The viscoelastic moduli increased by two orders of magnitude following photoirradiation. The values of G' and G'' at 10 rad s^{-1} before photoirradiation were 8.6×10^2 and 1.4×10^2 Pa, respectively, whereas those after photoirradiation (90% reaction completion) were 2.3×10^4 and 3.9×10^3 Pa, respectively. Ionogels containing azobenzene moieties in their polymer backbones exhibit photo-induced changes in their viscoelastic moduli of one order of magnitude or lower [36–38,44], whereas ionogels containing anthracene moieties in the polymer chain exhibit a larger change owing to photochemical crosslinking [43]. A significant change in the viscoelasticity was achieved in the current materials through a unique mechanism of structural transformation.

The shear-rate-dependence of the viscosities of **Gel-1** and **IL-1** [49] before and after photoirradiation is shown in Fig. 4b. Upon photoirradiation, their viscosities increased approximately 12 and 6 times, respectively, indicating more significant changes in the gel than in the pure IL. **IL-1** was a Newtonian fluid before and after photoirradiation, whereas **Gel-1** was a pseudoplastic fluid whose viscosity decreased at high shear rates owing to the collapse of the gel structure, approaching the value of **IL-1**.

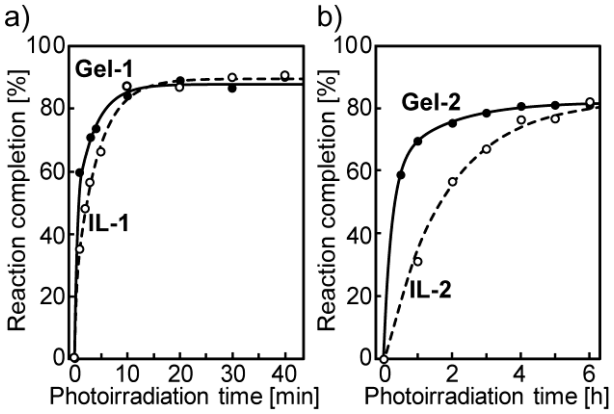

Fig. 3. Temporal evolution of the photoreactions of (a) **Gel-1** (●) and **IL-1** (○) [49], and (b) **Gel-2** (●) and **IL-2** (○) [48].

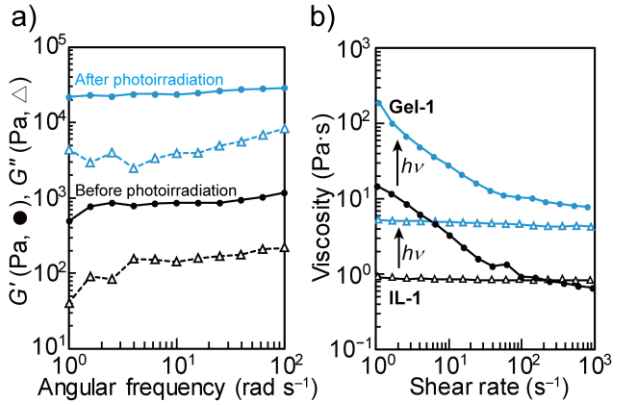

Fig. 4. (a) Angular frequency-dependence of the viscoelastic moduli of **Gel-1** (G': ●, G'': △) measured before (black) and after (blue) photoirradiation for 1 h at 25 °C (strain 0.1%). (b) Viscosities of **Gel-1** (●) and **IL-1** (△) [49] measured before (black) and after (blue) photoirradiation at 25 °C plotted as functions of shear rate.

*2.3. Reactivities of **Gel-2***

Pale yellow **Gel-2** transformed into a yellow rubber-like solid upon UV photoirradiation. The photochemical reaction required several hours, exhibiting a significantly lower rate of reaction than that of **Gel-1**. Upon heating, the photoproduct returned to its original gel form within 3 min. This reaction cycle was repeatable.

Upon UV photoirradiation, **Gel-2** turned into a yellow rubber-like solid within a few hours, in which the cations formed a coordination polymer structure, as shown in Fig. 1b. Fig. 3b shows the temporal evolution of the reaction, which was 60% complete at 30 min and 80% complete at 4 h, following which it nearly became constant, because the undissociated cations (~20%) were trapped inside the solid product [48]. The photochemical reaction was much slower than that of **Gel-1**, probably owing to the higher viscosity of **IL-2** than **IL-1** [49]. The evolution of the photoreaction of **IL-2** is shown in the figure as well. The photoreaction of **Gel-2** was much faster than that of liquid **IL-2**, which may be ascribed to efficient light scattering inside the gel. Heating the photoproduct at 120 °C for 3 min yielded the original ionogel. The thermal reverse reaction of the 3-D coordination polymer was slightly slower than that of **Gel-1** (Fig. S2b). The photoreaction and the thermal reaction constituted a repeatable cycle.

The viscoelastic moduli of **Gel-2** before and after photoirradiation are shown in Fig 5a. Prior to photoirradiation, G' exceeded G'' in the measured angular frequency region (strain 0.5%), which indicates elastic behavior. Photoirradiation for 4 h increased G' and G'' by approximately one and two orders of magnitude, respectively (80% reaction completion). G' and G'' measured at 10 rad s^{-1} before photoirradiation were 1.5×10^4 and 3.7×10^3 Pa, respectively, whereas those after photoirradiation were 4.1×10^5 and 2.4×10^5 Pa, respectively. The photoproduct exhibited elastic behavior ($G' > G''$) above approximately 5 rad s^{-1}, which indicates that the material is in the glass-rubber transition region. The viscoelastic moduli of the photoproduct are comparable to those of the photoproduct of **IL-2** ($G' = 4.7 \times 10^5$ Pa, $G'' = 2.0 \times 10^5$ Pa, at 10 rad s^{-1}), demonstrating that the gelator has a negligible effect on the viscoelastic moduli of the coordination polymer.

Upon heating the photoproduct at 120 °C for 10 min, the reverse reaction occurred to yield the original ionogel, and the viscoelastic moduli were restored (Fig 5a). The changes in

viscoelastic moduli at 10 rad s^{-1} during and after repeated photoirradiation and heating cycles are shown in Fig 5b, which shows that the viscoelasticity was repeatably controllable.

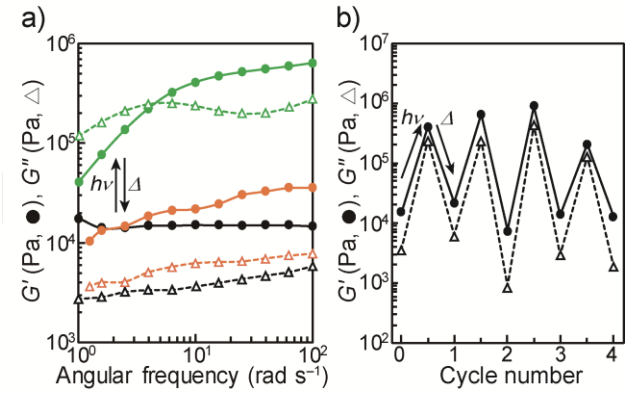

Fig 5. (a) Angular frequency-dependence of the viscoelastic moduli (*G′*: ●, *G″*: △) of **Gel-2** before (black) and after photoirradiation for 4 h (green), and after heating the photoproduct at 120 °C for 10 min (orange), measured at 25 °C, strain 0.5%. (b) Changes of viscoelastic moduli of **Gel-2** (*G′*: ●, *G″*: △) at 10 rad s^{-1} during repeated cycles of UV photoirradiation (4 h) and heating (120 °C for 10 min), measured at 25 °C, strain 0.5%.

*2.4. Ionic conductivities of **Gel-1** and **Gel-2***

The ionic conductivities of the gels were measured before and after UV photoirradiation. Photoirradiation of the gels leads to the formation of intermolecular coordination bonds, thereby decreasing the mobility of the cations, and the ionic conductivities of the gels are reversibly controlled by the application of light and heat.

The ionic conductivities of **Gel-1** and **Gel-2** at 25 °C were 2.6×10^{-4} and 2.5×10^{-5} S cm^{-1}, respectively (Table 1). These values are significantly lower than those of ionogels containing imidazolium ILs (*e.g.*, 4×10^{-1} S cm^{-1} for 1-allyl-3-butylimidazolium bis(trifluoromethanesulfonyl)amide/12-HSA) [58] because of the low ionic conductivities of the organometallic ILs (**IL-1**: 4.0×10^{-4} S cm^{-1}, **IL-2**: 3.0×10^{-5} S cm^{-1}) [49]. The ionic conductivities of the gels were only slightly lower than those of the pure constituent ILs,

whereas their viscosities were significantly higher (Fig S3), as typically observed in ionogels comprising low-molecular-weight gellators [17,58].

Upon photoirradiation, the ionic conductivity of **Gel-1** decreased by one order of magnitude from 2.6×10^{-4} to 1.2×10^{-5} S cm^{-1} in 30 min (Fig 6a). This is due to the oligomerization of the cations, which increases the viscosity of the liquid. The oligomer cations and FSA anions are the carrier ions, and the change in ionic conductivity is comparable to that of **IL-1**. In contrast, the ionic conductivity of **Gel-2** decreased by two orders of magnitude upon photoirradiation, from 2.5×10^{-5} to 3.3×10^{-7} S cm^{-1} in 3 h (Fig 6b). The change was larger than that of **Gel-1**, which is ascribed to the formation of the cation network, wherein the movement of the carrier ions (FSA anions and undissociated cations (~20%)) is significantly hampered in the photoproduct. Furthermore, the ionic conductivities of these gels following photoirradiation were slightly lower than those of the photoproducts of **IL-1** (3.7×10^{-5} S cm^{-1}) and **IL-2** (4.8×10^{-7} S cm^{-1}). In both cases, the ionic conductivity was restored following the heating of the photoproduct at 120 °C for 10 min; hence, the cycling of the ionic conductivity was repeatably controllable. These results further demonstrate that the responsivity can be tuned by the choice of IL in the gel, which is advantageous for device applications.

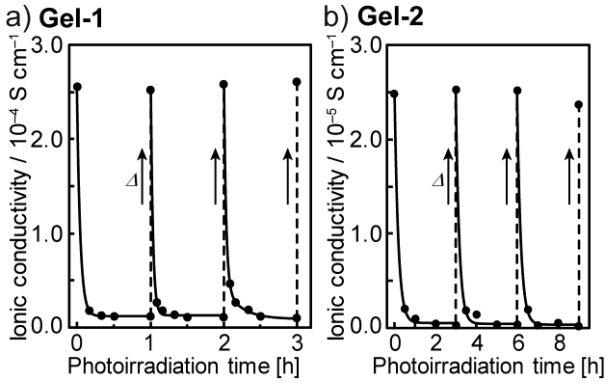

Fig 6. Ionic conductivity changes exhibited by (a) **Gel-1** and (b) **Gel-2**, measured at 25 °C during repeated cycles of UV photoirradiation and heating at 120 °C (10 min).

2.5. Temperature-dependence of Ionic Conductivity

The temperature-dependence of the ionic conductivity of the gels was measured before and after the photoreaction. The activation energies for ion transport increased following photoirradiation. The effect of the thermal reverse reaction on the conductivities was observed at elevated temperatures.

The ionic conductivities of **Gel-1** and **Gel-2** are shown in Fig 7 (left). As the temperature increased from 10 to 120 °C, their conductivities increased from 6.4×10^{-5} to 8.8×10^{-3} S cm^{-1}, and from 7.0×10^{-6} to 1.7×10^{-3} S cm^{-1}, respectively (Fig 7, left). No change was observed at the gel–sol transition temperature (73 °C), indicating that the gelator had little effect on the ionic conductivity. The Arrhenius plots deviated from a straight line, as is typically observed in ionogels [59], and the temperature-dependence $\sigma(T)$ obeyed the VFT (Vogel-Fulcher-Tamman) equation [60–62],

$$\sigma(T) = \frac{\mathrm{A}}{\sqrt{T}} \exp\left(\frac{-E_a}{k_B(T-T_0)}\right),$$

where A is proportional to the number of carrier ions in matrix, E_a and T_0 are the activation energy for ion transport and the ideal glass transition temperature, respectively [59,63]. The calculated values of the parameters are summarized in Table 1. The parameters A were similar for **Gel-1** and **Gel-2**, whereas their activation energies E_a differed at 75 and 122 meV, respectively. The higher activation energy for **Gel-2** is consistent with the higher viscosity of the IL in the gel. The activation energies were in the range typically observed from ionogels (50–150 meV) [59,64].

The temperature-dependence of the ionic conductivity of the ionogels following photoirradiation is shown in Fig 7 (right). During the heating process, the plots for the photoproducts of **Gel-1** and **Gel-2** were linear up to approximately 75 and 65 °C, respectively, and the ionic conductivities were lower than they were prior to photoirradiation. However, inflection points occurred at higher temperatures due to the thermal reverse reaction, and the

ionic conductivities became identical to those prior to the photoreaction. The change was continuous in the photoproduct of **Gel-1** because the photoproduct in the gel is in liquid state, whereas the photoproduct of **Gel-2** exhibited a somewhat discontinuous change between 75–120 °C, which is the thermal reaction temperature range of the photoproduct of **IL-2** [48]. In both cases, the ionic conductivities measured during cooling from 120 °C were identical to those of the original ionogels.

The temperature-dependences of the ionic conductivities of the photoproducts were fitted using the Arrhenius equation $\sigma(T) = \sigma_\infty \exp(-E_a/k_B T)$ [65,66]. The plots are straight lines and not well fitted using the VFT equation. The calculated values of the parameters are summarized in Table 1. The activation energies E_a for **Gel-1** and **Gel-2** after photoirradiation were 992 and 780 meV, respectively, which are much higher than the values exhibited prior to the photoreaction, reflecting the formation of intermolecular coordination bonds. The σ_∞ value of **Gel-1** (3.2×10^{11} S cm^{-1}) was much higher than that of **Gel-2** (1.4×10^{7} S cm^{-1}) after photoirradiation, because the cation oligomer can be a carrier ion, whereas the coordination polymer cation is immobile. However, these analyses are tentative because the photoproducts were in a transient thermal state, and their actual conduction mechanism is complex.

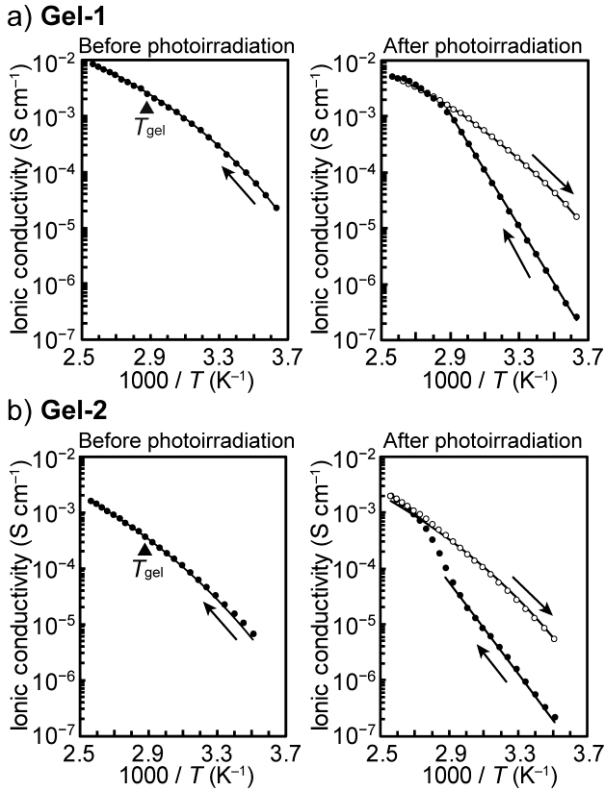

Fig 7. Temperature-dependence of the ionic conductivities of (a) **Gel-1**, (b) **Gel-2**, and their photoproducts (●: heating, ○: cooling). The conductivities of the photoproducts were initially measured up to 120 °C, that temperature was maintained for 10 min, and subsequent measurements were performed during cooling.

Table 1. Ionic conductivities of **Gel-1** and **Gel-2** before and after UV photoirradiation, and the parameters for their temperature-dependence

Compounds		$\sigma_{25\,°C}$ (S cm^{-1})	E_a (meV)	A (S K$^{1/2}$ cm^{-1})[a]	T_0 (K)[a]	σ_∞ (S cm^{-1})[b]
Gel-1	before photoirradiation	2.6×10^{-4}	74.9	19.1(3.9)	186.9(6.4)	
	after photoirradiation (30 min)	1.2×10^{-5}	992			$3.2(0.4) \times 10^{11}$
Gel-2	before photoirradiation	2.5×10^{-5}	122	17.0(2.2)	166.3(3.1)	
	after photoirradiation (3 h)	3.3×10^{-7}	780			$1.4(0.5) \times 10^{7}$

[a]Parameters for the VFT equation. [b]Parameters for the Arrhenius equation. Values in parentheses are standard deviations.

3. Conclusion

Photoreactive ionogels containing organometallic ionic liquids were developed, and their ionic conductivities and viscoelasticities could be reversibly controlled by the application of

UV light and heat. This controllability originates from the reversible structural transformation of the photoreactive ILs in the gel. Transformations between gels with different viscoelasticities or between gels and rubber-like solids were achieved depending on the substituents of the ILs, and the resulting change in the ionic conductivity was very large. This study demonstrated a novel strategy for fabricating stimuli-responsive ionically conducting gels. Ionogels such as the ones developed in this work can act as photoswitchable solid electrolytes, which may facilitate the development of novel electronic devices. Although a low-molecular-weight gelator was used in this study, physical gelators whose properties can be tuned in a wider range can be applied in its place. These investigations are currently underway in our laboratory.

4. Experimental

4.1. General Considerations

$[Ru(C_5H_5)(C_6H_5OC_3H_6CN)]FSA$ (**IL-1**) [55] and $[Ru(C_5H_5)\{1,3,5\text{-}C_6H_3(OC_6H_{12}CN)_3\}]FSA$ (**IL-2**) [48] were synthesized according to previously reported methods. ^1H nuclear magnetic resonance (NMR) spectra were recorded using a Bruker Avance 400 spectrometer. Fourier-transform infrared (FT-IR) spectra were acquired using a Thermo Nicolet iS5 spectrometer fitted with an attenuated total reflectance (ATR). UV-vis absorption spectra were recorded on a JASCO V-570 UV/VIS/NIR spectrophotometer. Differential scanning calorimetry (DSC) measurements were performed using a TA Instruments Q100 differential scanning calorimeter at a sweep rate of 10 K min^{-1}. Dynamic viscoelasticities were measured using a TA Instruments DHR-1 rheometer equipped with an 8 mm parallel plate. The frequency-dependence of the dynamic viscoelasticity was measured at 25 °C. The ionic conductivities were measured using a Solartron 1260 impedance analyzer. The ionogels were sandwiched between gold interdigitated electrodes (gap dimension: 200 μm) and quartz glass

plates, which were further sealed with epoxy resin. The Japan High Tech heating/cooling stage 10013L was used for temperature control.

4.2. Preparation and Reaction

Gel-1 and **Gel-2** were prepared by dissolving **IL-1** and **IL-2** (20 mg), respectively, with 12-hydroxyoctadecanoic acid (1 mg) in dichloromethane (1.5 mL), followed by heating at 90 °C to evaporate the solvent. The sample was subsequently heated at 120 °C for 10 min and allowed to cool to ambient temperature. The gel obtained was dried in vacuum for 12 h. UV photoirradiation experiments were conducted on samples sandwiched between two quartz plates at 10 °C. The sealed electrodes were photoirradiated for ionic conductivity measurements. A Hamamatsu LIGHTNINGCURE LC-L1V5 UV-LED (365 nm, 600 mW cm^{-2}) was used as the light source. Thermal reactions were performed inside a preheated oven, and measurements were performed after standing the samples at room temperature for 15 h. The dissociation rates of the cations in the photoproducts were determined from the ratio of $[Ru(C_5H_5)(NCCD_3)_3]^+$ and the remaining sandwich complex in the ^1H NMR spectra (CD_3CN). The experimental error for the dynamic viscoelasticity measurements (Fig. 5b) was large because the sample was unloaded and reloaded after each cycle. The photoirradiation and heating cycles were performed under an argon atmosphere.

CRediT authorship contribution statement

Ryo Sumitani: Investigation, Visualization, Writing - original draft. **Tomoyuki Mochida:** Conceptualization, Writing - original draft.

Funding

This work was supported financially by KAKENHI (grant number: 20H02756) from the Japan

Society for the Promotion of Science (JSPS) and Grant-in-Aid for JSPS Research Fellow (grant number: 21J12056).

Graphical abstract

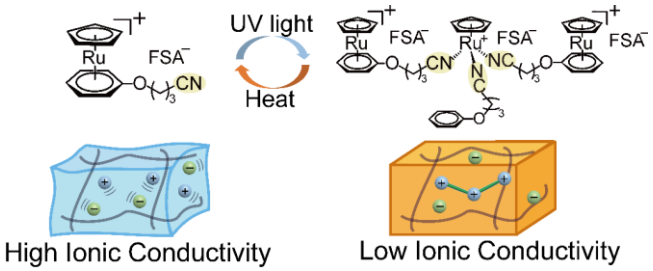

Ionogels composed of photoreactive organometallic ionic liquids and a low-molecular-weight gelator were prepared. These gels reversibly transformed into a gel having higher viscoelasticity or a rubber-like solid upon application of light and heat, thereby enabling reversible control of their ionic conductivity and viscoelasticity.

- Ionogels containing photoreactive organometallic ionic liquids were prepared.
- The gels were repeatedly hardened and softened by application of light and heat.
- The ionic conductivities of the gels were reversibly controlled using light and heat.

References

[1] Kar, M.; Matuszek, K.; MacFarlane, D. R. Ionic Liquids, In *Kirk–Othmer Encyclopedia of Chemical Technology*; John Wiley & Sons, Inc., **2019**. https://doi.org/10.1002/0471238961.ionisedd.a01.pub2

[2] Lee, S. Y.; Ogawa, A.; Kanno, M.; Nakamoto, H.; Yasuda, T.; Watanabe, M. Nonhumidified Intermediate Temperature Fuel Cells Using Protic Ionic Liquids. *J. Am. Chem. Soc.* **2010**, *132*, 9764–9773. https://doi.org/10.1021/ja102367x

[3] Devanathan, R. Recent Developments in Proton Exchange Membranes for Fuel Cells. *Energy Environ. Sci.* **2008**, *1*, 101–119. https://doi.org/10.1039/B808149M

[4] Wishart, J. F. Energy Applications of Ionic Liquids. *Energy Environ. Sci.* **2009**, *2*, 956–961. https://doi.org/10.1039/B906273D

[5] Javed, F.; Ullah, F.; Zakaria, M. R.; Akil, H. M. An Approach to Classification and Hi-Tech Applications of Room-Temperature Ionic Liquids (RTILs): A Review. *J. Mol. Liq.* **2018**, *271*, 403–420. https://doi.org/10.1016/j.molliq.2018.09.005

[6] Watanabe, M.; Thomas, M. L.; Zhang, S.; Ueno, K.; Yasuda, T.; Dokko, K. Application of Ionic Liquids to Energy Storage and Conversion Materials and Devices. *Chem. Rev.* **2017**, *117*, 7190–7239. https://doi.org/10.1021/acs.chemrev.6b00504

[7] Zhan, T.; Tian, X.; Ding, G.; Liu, X.; Wang, L.; Teng, H. Quaternarization Strategy to Ultrathin Lamellar Graphitic C3N4 Ionic Liquid Nanostructure for Enhanced Electrochemical 2,4-Dichlorophenol Sensing. *Sens. Actuators, B* **2019**, *283*, 463–471. https://doi.org/10.1016/j.snb.2018.12.068

[8] Le Bideau, J.; Viau, L.; Vioux, A. Ionogels, Ionic Liquid Based Hybrid Materials. *Chem. Soc. Rev.* **2011**, *40*, 907–925. https://doi.org/10.1039/C0CS00059K

[9] Zhang, D.-Z.; Ren, Y.-Y.; Hu, Y.; Li, L.; Yan, F. Ionic Liquid/Poly(ionic liquid)-based Semi-solid State Electrolytes for Lithium-ion Batteries. *Chin. J. Polym. Sci.* **2020**, *38*, 506–513. https://doi.org/10.1007/s10118-020-2390-1

[10] Vioux, A.; Viau, L.; Volland, S.; Le Bideau, J. Use of Ionic Liquids in Sol-Gel; Ionogels and Applications. *C. R. Chim.* **2010**, *13*, 242–255. https://doi.org/10.1016/j.crci.2009.07.002

[11] Chen, N.; Zhang, H.; Li, L.; Chen, R.; Guo, S. Ionogel Electrolytes for High-Performance Lithium Batteries: A Review. *Adv. Energy Mater.* **2018**, *8*, 1702675. https://doi.org/10.1002/aenm.201702675

[12] Shaplov, A. S.; Marcilla, R.; Mecerreyes, D. Recent Advances in Innovative Polymer

Electrolytes based on Poly(ionic liquid)s. *Electrochim. Acta* **2015**, *175*, 18−34. https://doi.org/10.1016/j.electacta.2015.03.038

[13] Yuan, J.; Mecerreyes, D.; Antonietti, M. Poly(ionic liquid)s: An update. *Prog. Polym. Sci.* **2013**, *38*, 1009−1036. https://doi.org/10.1016/j.progpolymsci.2013.04.002

[14] Yuan, J.; Antonietti, M. Poly(ionic liquid)s: Polymers Expanding Classical Property Profiles. *Polymer* **2011**, *52*, 1469−1482. https://doi.org/10.1016/j.polymer.2011.01.043

[15] Mecerreyes, D. Polymeric Ionic Liquids: Broadening the Properties and Applications of Polyelectrolytes. *Prog. Polym. Sci.* **2011**, *36*, 1629−1648. https://doi.org/10.1016/j.progpolymsci.2011.05.007

[16] Kimizuka, N.; Nakashima, T. Spontaneous Self-Assembly of Glycolipid Bilayer Membranes in Sugar-philic Ionic Liquids and Formation of Ionogels. *Langmuir* **2001**, *17*, 6759–6761. https://doi.org/10.1021/la015523e

[17] Hanabusa, K.; Fukui, H.; Suzuki, M.; Shirai, H. Specialist Gelator for Ionic Liquids. *Langmuir* **2005**, *21*, 10383–10390. https://doi.org/10.1021/la051323h

[18] Tu, T.; Bao, X.; Assenmacher, W.; Peterlik, H.; Daniels, J.; Dötz, K. H. Efficient Air-Stable Organometallic Low-Molecular-Mass Gelators for Ionic Liquids: Synthesis, Aggregation and Application of Pyridine-Bridged Bis(benzimidazolylidene)-Palladium Complexes. *Chem. - Eur. J.* **2009**, *15*, 1853–1861. https://doi.org/10.1002/chem.200802116

[19] Dutta, S.; Das, D.; Dasgupta, A.; Das, P. K. Amino Acid Based Low-Molecular-Weight Ionogels as Efficient Dye-Adsorbing Agents and Templates for the Synthesis of TiO_2 Nanoparticles. *Chem. - Eur. J.* **2010**, *16*, 1493–1505. https://doi.org/10.1002/chem.200901917

[20] Minakuchi, N.; Hoe, K.; Yamaki, D.; Ten-No, S.; Nakashima, K.; Goto, M.; Mizuhata, M.; Maruyama, T. Versatile Supramolecular Gelators That Can Harden Water, Organic Solvents and Ionic Liquids. *Langmuir* **2012**, *28*, 9259–9266. https://doi.org/10.1021/la301442f

[21] Ishioka, Y.; Minakuchi, N.; Mizuhata, M.; Maruyama, T. Supramolecular Gelators Based

on Benzenetricarboxamides for Ionic Liquids. *Soft Matter* **2014**, *10*, 965–971. https://doi.org/10.1039/C3SM52363B

[22] Li, D. M.; Shi, F.; Guo, S.; Deng, Y. Q. One-Pot Synthesis of Silica Gel Confined Functional Ionic Liquids: Effective Catalysts for Deoximation under Mild Conditions. *Tetrahedron Lett.* **2004**, *45*, 265–268. https://doi.org/10.1016/j.tetlet.2003.10.175

[23] Néouze, M.-A.; Le Bideau, J.; Gaveau, P.; Bellayer, S.; Vioux, A. Ionogels, New Materials Arising from the Confinement of Ionic Liquids within Silica-Derived Networks. *Chem. Mater.* **2006**, *18*, 3931–3936. https://doi.org/10.1021/cm060656c

[24] Noro, A.; Matsushima, S.; He, X.; Hayashi, M.; Matsushita, Y. Thermoreversible Supramolecular Polymer Gels via Metal–Ligand Coordination in an Ionic Liquid. *Macromolecules* **2013**, *46*, 8304–8310. https://doi.org/10.1021/ma401820x

[25] Sinawang, G.; Kobayashi, Y.; Zheng, Y.; Takashima, Y.; Harada, A.; Yamaguchi, H. Preparation of Supramolecular Ionic Liquid Gels Based on Host–Guest Interactions and Their Swelling and Ionic Conductive Properties. *Macromolecules* **2019**, *52*, 2932–2938. https://doi.org/10.1021/acs.macromol.8b02395

[26] Snedden, P.; Cooper, A. I.; Scott, K.; Winterton, N. Cross-Linked Polymer-Ionic Liquid Composite Materials. *Macromolecules* **2003**, *36*, 4549–4556. https://doi.org/10.1021/ma021710n

[27] Klingshirn, M. A.; Spear, S. K.; Subramanian, R.; Holbrey, J. D.; Huddleston, J. G.; Rogers, R. D. Gelation of Ionic Liquids Using a Cross-Linked Poly(Ethylene Glycol) Gel Matrix. *Chem. Mater.* **2004**, *16*, 3091–3097. https://doi.org/10.1021/cm0351792

[28] Lee, H. Y.; Cai, Y.; Velioglu, S.; Mu, C.; Chang, C. J.; Chen, Y. L.; Song, Y.; Chew, J. W.; Hu, X. M. Thermochromic Ionogel: A New Class of Stimuli Responsive Materials with Super Cyclic Stability for Solar Modulation. *Chem. Mater.* **2017**, *29*, 6947–6955. https://doi.org/10.1021/acs.chemmater.7b02402

[29] Benito-Lopez, F.; Antoñana-Díez, M.; Curto, V. F.; Diamond, D.; Castro-López, V. Modular Microfluidic Valve Structures Based on Reversible Thermoresponsive Ionogel Actuators. *Lab Chip* **2014**, *14*, 3530–3538. https://doi.org/10.1039/C4LC00568F

[30] Gil-González, N.; Akyazi, T.; Castaño, E.; Benito-Lopez, F.; Morant-Miñana, M. C. Elucidating the Role of the Ionic Liquid in the Actuation Behavior of Thermo-Responsive Ionogels. *Sens. Actuators, B* **2018**, *260*, 380–387. https://doi.org/10.1016/j.snb.2017.12.153

[31] Zhang, Y.-D; Fan, X.-H; Shen, Z.; Zhou, Q.-F. Thermoreversible Ion Gel with Tunable Modulus Self-Assembled by a Liquid Crystalline Triblock Copolymer in Ionic Liquid. *Macromolecules* **2015**, *48*, 4927–4935. https://doi.org/10.1021/acs.macromol.5b01103

[32] Hall, C. C.; Zhou, C.; Danielsen, S. P. O.; Lodge, T. P. Formation of Multicompartment Ion Gels by Stepwise Self-Assembly of a Thermoresponsive ABC Triblock Terpolymer in an Ionic Liquid. *Macromolecules* **2016**, *49*, 2298–2306. https://doi.org/10.1021/acs.macromol.5b02789

[33] Yang, F.; Wu, D.; Luo, Z.; Tan, B.; Xie, Z. Hybrid Organic-Inorganic Dyeionogels: Reversibly pH-Responsive Materials Based Dye-Ionic Liquids with Improved Structural Stability and Flexibility. *Sens. Actuators, B* **2017**, *249*, 486–492. https://doi.org/10.1016/j.snb.2017.04.133

[34] Xie, Z.-L.; Huang, X.; Taubert, A. DyeIonogels: Proton-Responsive Ionogels Based on a Dye-Ionic Liquid Exhibiting Reversible Color Change. *Adv. Funct. Mater.* **2014**, *24*, 2837–2843. https://doi.org/10.1002/adfm.201303016

[35] Kavanagh, A.; Byrne, R.; Diamond, D.; Radu, A. A Two-Component Polymeric Optode Membrane Based on a Multifunctional Ionic Liquid. *Analyst* **2011**, *136*, 348–353. https://doi.org/10.1039/C0AN00770F

[36] Ueki, T.; Nakamura, Y.; Usui, R.; Kitazawa, Y.; So, S.; Lodge, T. P.; Watanabe, M. Photoreversible Gelation of a Triblock Copolymer in an Ionic Liquid. *Angew. Chem.* **2015**, *127,*

3061–3065. https://doi.org/10.1002/ange.201411526

[37] Wang, C.; Hashimoto, K.; Tamate, R.; Kokubo, H.; Morishima, K.; Li, X.; Shibayama, M.; Lu, F.; Nakanishi, T.; Watanabe, M. Viscoelastic Change of Block Copolymer Ion Gels in a Photo-Switchable Azobenzene Ionic Liquid Triggered by Light. *Chem. Commun.* **2019**, *55*, 1710–1713. https://doi.org/10.1039/C8CC08203K

[38] Wang, C.; Hashimoto, K.; Tamate, R.; Kokubo, H.; Watanabe, M. Controlled Sol-Gel Transitions of a Thermoresponsive Polymer in a Photoswitchable Azobenzene Ionic Liquid as a Molecular Trigger. *Angew. Chem., Int. Ed.* **2018**, *57*, 227–230. https://doi.org/10.1002/anie.201710288

[39] Czugala, M.; O'Connell, C.; Blin, C.; Fischer, P.; Fraser, K. J.; Benito-Lopez, F.; Diamond, D. Swelling and Shrinking Behaviour of Photoresponsive Phosphonium-Based Ionogel Microstructures. *Sens. Actuators, B* **2014**, *194*, 105–113. https://doi.org/10.1016/j.snb.2013.12.072

[40] Benito-Lopez, F.; Byrne, R.; Răduţă, A. M.; Vrana, N. E.; McGuinness, G.; Diamond, D. Ionogel-Based Light-Actuated Valves for Controlling Liquid Flow in Micro-Fluidic Manifolds. *Lab Chip* **2010**, *10*, 195–201. https://doi.org/10.1039/B914709H

[41] Tamada, M.; Watanabe, T.; Horie, K.; Ohno, H. Control of Ionic Conductivity of Ionic Liquid/Photoresponsive Poly(amide acid) Gels by Photoirradiation. *Chem. Commun.* **2007**, 4050–4052. https://doi.org/10.1039/B705060G

[42] Wang, C.; Dong, W.; Li, P.; Wang, Y.; Tu, H.; Tan, S.; Wu, Y.; Watanabe, M. Reversible Ion-Conducting Switch by Azobenzene Molecule with Light-Controlled Sol–Gel Transitions of the PNIPAm Ion Gel. *ACS Appl. Mater. Interfaces* **2020**, *12*, 42202–42209. https://doi.org/10.1021/acsami.0c12910

[43] Saruwatari, A.; Tamate, R.; Kokubo, H.; Watanabe, M. Photohealable Ion Gels Based on the Reversible Dimerisation of Anthracene. *Chem. Commun.* **2018**, *54*, 13371–13374.

https://doi.org/10.1039/C8CC07775D

[44] Ueki, T.; Usui, R.; Kitazawa, Y.; Lodge, T. P.; Watanabe, M. Thermally Reversible Ion Gels with Photohealing Properties Based on Triblock Copolymer Self-Assembly. *Macromolecules* **2015**, *48*, 5928–5933. https://doi.org/10.1021/acs.macromol.5b01366

[45] Cao, Z.; Liu, H.; Jiang, L. Hydrogen-Bonding-Driven Tough Ionogels Containing Spiropyran-Functionalized Ionic Liquids. *ACS Appl. Polym. Mater.* **2020**, *2*, 2359–2365. https://doi.org/10.1021/acsapm.0c00297

[46] Jiang, W.; Hao, J.; Wu, Z. Anisotropic Ionogels of Sodium Laurate in a Room-Temperature Ionic Liquid. *Langmuir* **2008**, *24*, 3150–3156. https://doi.org/10.1021/la703632g

[47] Xie, Z.-L.; Jeličić, A.; Wang, F.-P.; Rabu, P.; Friedrich, A.; Beuermann, S.; Taubert, A. Transparent, Flexible, and Paramagnetic Ionogels Based on PMMA and the Iron-Based Ionic Liquid 1-Butyl-3-methylimidazolium tetrachloroferrate(III) [Bmim][$FeCl_4$]. *J. Mater. Chem.* **2010**, *20*, 9543–9549. https://doi.org/10.1039/C0JM01733G

[48] Funasako, Y.; Mori, S.; Mochida, T. Reversible Transformation between Ionic Liquids and Coordination Polymers by Application of Light and Heat. *Chem. Commun.* **2016**, *52*, 6277–6279. https://doi.org/10.1039/C6CC02807A

[49] Sumitani, R.; Yoshikawa, H.; Mochida, T. Reversible Control of Ionic Conductivity and Viscoelasticity of Organometallic Ionic Liquids by Application of Light and Heat. *Chem. Commun.* **2020**, *56*, 6189–6192. https://doi.org/10.1039/D0CC02786C

[50] Ueda, T.; Tominaga, T.; Mochida, T.; Takahashi, K.; Kimura, S. Photogeneration of Microporous Amorphous Coordination Polymers from Organometallic Ionic Liquids. *Chem. - Eur. J.* **2018**, *24*, 9490–9493. https://doi.org/10.1002/chem.201801365

[51] Sumitani, R.; Mochida, T. Reversible Formation of Soft Coordination Polymers from Liquid Mixtures of Photoreactive Organometallic Ionic Liquid and Bridging Molecules. *Soft Matter*, **2020**, *16*, 9946–9954. https://doi.org/10.1039/D0SM01567A

[52] Sumitani, R.; Mochida, T. Metal-Containing Poly(ionic liquid) Exhibiting Photogeneration of Coordination Network: Reversible Control of Viscoelasticity and Ionic Conductivity. *Macromolecules* **2020**, *53*, 6968–6974. https://doi.org/10.1021/acs.macromol.0c01141

[53] Hughes, N. E.; Marangoni, A. G.; Wright, A. J.; Rogers, M. A.; Rush, J. W. E. Potential Food Applications of Edible Oil Organogels. *Trends Food Sci. Technol.* **2009**, *20*, 470–480. https://doi.org/10.1016/j.tifs.2009.06.002

[54] Voss, B. A.; Bara, J. E.; Gin, D. L.; Noble, R. D. Physically Gelled Ionic Liquids: Solid Membrane Materials with Liquidlike CO_2 Gas Transport. *Chem. Mater.* **2009**, *21*, 3027–3029. https://doi.org/10.1021/cm900726p

[55] Komurasaki, A.; Funasako, Y.; Mochida, T. Colorless Organometallic Ionic Liquids from Cationic Ruthenium Sandwich Complexes: Thermal Properties, Liquid Properties, and Crystal Structures of $[Ru(\eta^5\text{-}C_5H_5)(\eta^6\text{-}C_6H_5R)][X]$ (X = $N(SO_2CF_3)_2$, $N(SO_2F)_2$, PF_6). *Dalton Trans.* **2015**, *44*, 7595–7605. https://doi.org/10.1039/C5DT00723B

[56] Takeno, H.; Maehara, A.; Kuchiishi, M.; Yoshiba, K.; Takeshita, H.; Kondo, S.; Dobashi, T.; Takenaka, M.; Hasegawa, H. Structural and Thermal Properties of Unpurified and Purified 12-Hydroxystearic Acid Solutions. *Sen'i Gakkaishi* **2012**, *68*, 248–252. https://doi.org/10.2115/fiber.68.248

[57] Yamamuro, O.; Minamimoto, Y.; Inamura, Y.; Hayashi, S.; Hamaguchi, H. Heat Capacity and Glass Transition of an Ionic Liquid 1-Butyl-3-methylimidazolium chloride. *Chem. Phys. Lett.* **2006**, *423*, 371–375. https://doi.org/10.1016/j.cplett.2006.03.074

[58] Takeno, H.; Kozuka, M. Effects of Cooling Rates on Self-Assembling Structures of 12-Hydroxystearic Acid in an Ionic Liquid. *Adv. Mater. Sci. Eng.* **2017**, *2017*, 1–8. https://doi.org/10.1155/2017/4762379

[59] Matsumi, N.; Nakamura, Y.; Aoi, K.; Watanabe, T.; Mizumo, T.; Ohno, H. Enhanced Ionic

Conduction in Organoboron Ion Gels Facilely Designed *via* Condensation of Cellulose with Boric Acids in Ionic Liquids. *Polym. J.* **2009**, *41*, 437–441. https://doi.org/10.1295/polymj.PJ2008289

[60] Vogel, H. The Law of the Relationship between Viscosity of Liquids and the Temperature. *Phys. Z.* **1921**, *22*, 645–646.

[61] Fulcher, G. S. Analysis of Recent Measurements of the Viscosity of Glasses. *J. Am. Ceram. Soc.* **1925**, *8*, 339–355. https://doi.org/10.1111/j.1151-2916.1925.tb16731.x

[62] Tammann, G.; Hesse, W. Die Abhängigkeit der Viscosität von der Temperatur bie unterkühlten Flüssigkeiten. *Allg. Chemie* **1926**, *156*, 245–257. https://doi.org/10.1002/zaac.19261560121

[63] Vila, J.; Ginés, P.; Pico, J. M.; Franjo, C.; Jiménez, E.; Varela, L. M.; Cabeza, O. Temperature Dependence of the Electrical Conductivity in EMIM-Based Ionic Liquids: Evidence of Vogel–Tamman–Fulcher behavior. *Fluid Phase Equilib.* **2006**, *242*, 141–146. https://doi.org/10.1016/j.fluid.2006.01.022

[64] Ashby, D. S.; DeBlock, R. H.; Lai, C.-H.; Choi, C. S.; Dunn, B. S. Patternable, Solution-Processed Ionogels for Thin-Film Lithium-Ion Electrolytes. *Joule* **2017**, *1*, 344–358. https://doi.org/10.1016/j.joule.2017.08.012

[65] Petrowsky, M.; Frech, R. Application of the compensated Arrhenius formalism to self-diffusion: implications for ionic conductivity and dielectric relaxation. *J. Phys. Chem. B* **2010**, *114*, 8600–8605. https://doi.org/10.1021/jp1020142

[66] Every, H.; Bishop, A. G.; Forsyth, M.; MacFarlane, D. R. Ion diffusion in molten salt mixtures. *Electrochim. Acta* **2000**, *45*, 1279–1284. https://doi.org/10.1016/S0013-4686(99)00332-1

Supporting Information

Switchable Ionic Conductivity and Viscoelasticity of Ionogels Containing Photo- and Thermo-Responsive Organometallic Ionic Liquids

Ryo Sumitani[a] and Tomoyuki Mochida*[a,b]

[a]*Department of Chemistry, Graduate School of Science, Kobe University, 1-1 Rokkodai, Nada, Kobe, Hyogo 657-8501, Japan. E-mail: tmochida@platinum.kobe-u.ac.jp*

[b]*Center for Membrane and Film Technology, Kobe University, 1-1 Rokkodai, Nada, Kobe, Hyogo 657-8501, Japan*

Fig. S1. DSC traces of (a) **Gel-1** and (b) **Gel-2**.

Fig. S2. Temporal evolutions of the reactions undergone by **Gel-1** (●) and **Gel-2** (○) upon heating at 120 °C.

Fig. S3. Photographs of (a) **Gel-1** and (b) **Gel-2** before and after photoirradiation.

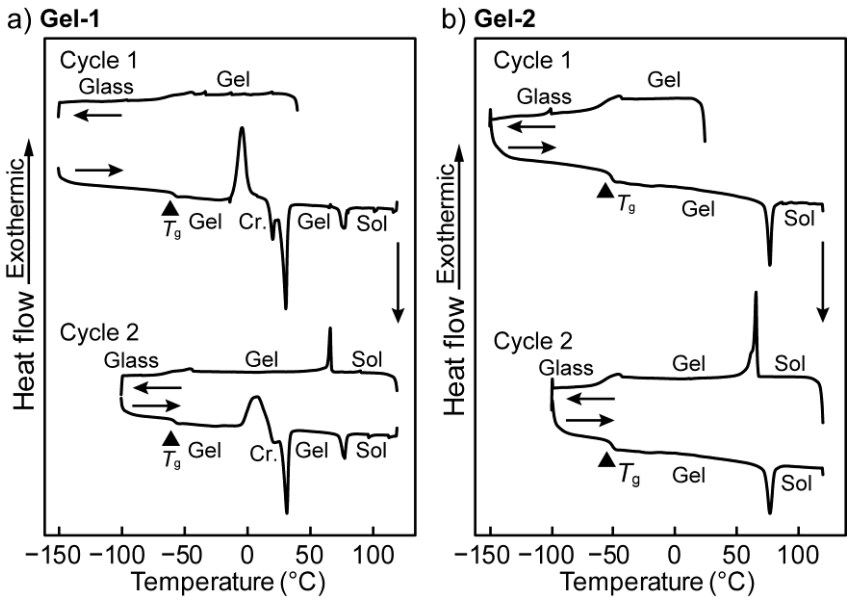

Fig. S1. DSC traces of (a) **Gel-1** and (b) **Gel-2**.

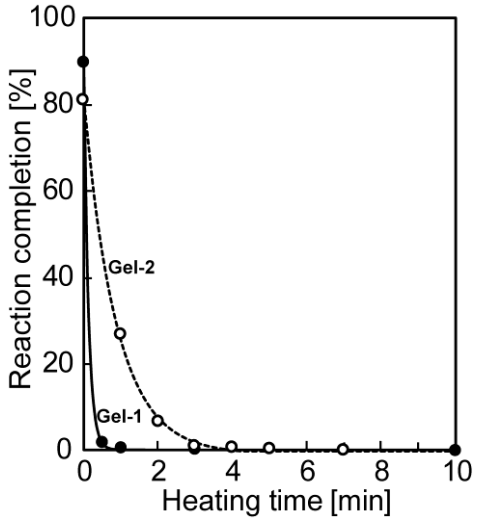

Fig. S2. Temporal evolutions of the reactions undergone by **Gel-1** (●) and **Gel-2** (○) upon heating at 120 °C.

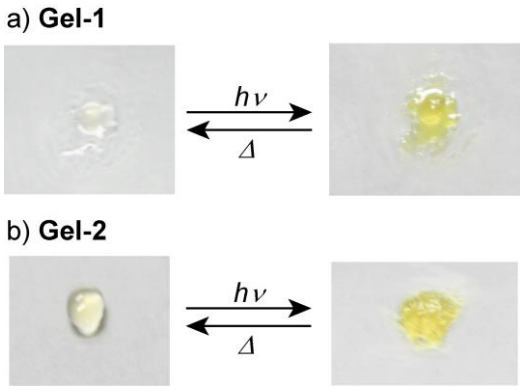

Fig. S3. Photographs of (a) **Gel-1** and (b) **Gel-2** before and after photoirradiation.